chemistry proceedings

MDPI

Proceeding Paper

Greener Synthesis, In-Silico and Theoretical Analysis of Hydrazides as Potential Antituberculosis Agents (Part 1) †

Suraj N. Mali [1,*], Anima Pandey [1], Bapu R. Thorat [2] and Chin-Hung Lai [3]

[1] Department of Pharmaceutical Sciences and Technology, Birla Institute of Technology, Mesra, Ranchi 835215, India; phdph10006.20@bitmesra.ac.in
[2] Department of Chemistry, Government College of Arts and Science, Aurangabad 431004, India; apandey@bitmesra.ac.in
[3] Department of Medical Applied Chemistry, Chung Shan Medical University, Taichung 40241, Taiwan; bthorat78@gmail.com
* Correspondence: mali.suraj1695@gmail.com
† Presented at the 25th International Electronic Conference on Synthetic Organic Chemistry, 15–30 November 2021; Available online: https://ecsoc-25.sciforum.net/.

Abstract: Since several decades, our healthcare burden has been increased due to tremendous cases of multidrug-resistant (MDR-TB) and extensively drug-resistant tuberculosis (XDR-TB) infections, especially in tropical countries. In the present study, we have synthesized ten hydrazides with the use of the greener Chitosan-derived catalyst. This catalyst accomplished the said condensation reaction within 15–30 min at room temperature conditions. All our synthesized compounds showed stronger affinities against *Mycobacterium tb* and bacterial targets, especially towards 1d7u, than the standard drug ciprofloxacin. One of our compounds retained a lower toxicity (electrophilicity index (ω) 3.1304), low chemical hardness (η: 2.1740), and high softness (S: 0.4600). In the realm of the development of more potent, effective, and safe antituberculosis agents with an effective greener synthesis, our current study would provide more insights on potent analogues containing hydrazine motifs in them.

Keywords: hydrazide-hydrazones; antituberculosis activity; in-silico analysis; tuberculosis; synthesis; molecular modelling

check for updates

Citation: Mali, S.N.; Pandey, A.; Thorat, B.R.; Lai, C.-H. Greener Synthesis, In-Silico and Theoretical Analysis of Hydrazides as Potential Antituberculosis Agents (Part 1). *Chem. Proc.* **2022**, *8*, 86. https://doi.org/10.3390/ecsoc-25-11655

Academic Editor: Julio A. Seijas

Published: 13 November 2021

1. Introduction

Antimicrobial resistance is a severe global healthcare threat, which is hampering the quality of human life [1–4]. Searching for potent, safe, and effective agents is still a difficult task for medicinal chemists all over the world. Tuberculosis (TB) remains a major global healthcare threat, as reported in WHO in 2019 [4]. Hydrazide–hydrazones motifs were reported for their wider pharmacological potentials, such as being anticonvulsant, anticancer, antiviral, etc. [4]. Recently, computational methodologies are also gaining tremendous attention by medicinal chemists [4–24]. Recent applications of the Chitosan catalyst have been elaborated thoroughly, and the relevant literatures are cited in references [25–29].

Considering the stronger antimicrobial potentials of Hydrazide–hydrazones having the azomethine group (–NH–N=CH–), we decided to synthesize newer hydrazides using a greener catalyst, *Chitosan hydrochloride*, and theoretically tested (**3a**–**3j**) for their antimicrobial potentials using several computational approaches [5]. These attempts would also enlighten us on the probable anti-TB mechanisms of previously (in vitro) tested hydrazides [6–24] (Figure 1). Moreover, recently, our group has also reported anti-TB potentials of a variety of potent Hydrazide–hydrazone derivatives.

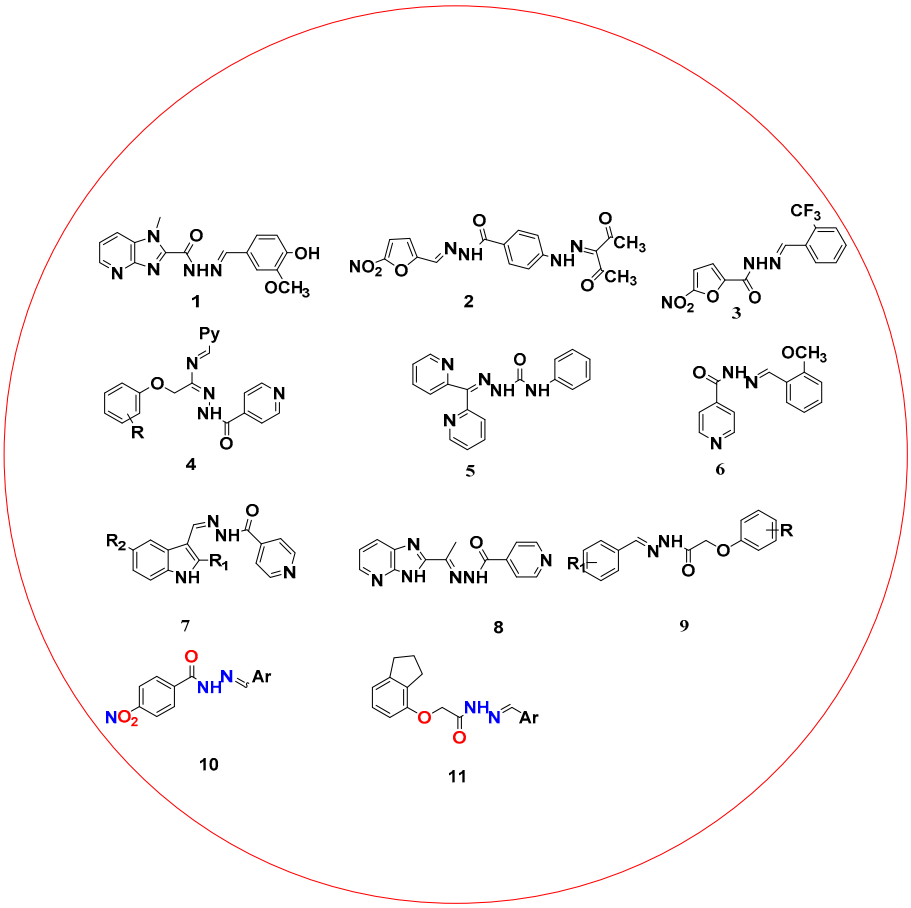

Figure 1. Schematic representation of some literature-reported bioactive molecules.

2. Materials and Methods

All the necessary chemicals required for Figure 2 were procured from Sigma-Aldrich and Merck (Mumbai, India). Raw chitosan (MW = 50,000–190,000 Dalton) was purchased from Sigma-Aldrich. All compounds were synthesized according to the previous literature and characterized once again using various spectroscopic techniques, like proton magnetic resonance (1H-NMR), FT-IR (Infrared spectroscopy), etc. Exhaustive details on catalyst characterization and methods are provided in the supporting information, and the data is coherent with the previous literature.

2.1. Preparation of Chitosan-HCl Catalyst

We synthesized the new chitosan-HCl catalyst by taking raw chitosan (1 g) and allowing it to dissolve in 75 cm^3 of 1% HCl. The stirring rate was maintained at 800 rpm, along with frequent heating at 40 °C. Furthermore, the mixture was allowed to pass through cotton to filter undissolved mass. Finally, filtrate was collected and dried to obtain the catalyst [5].

2.2. Synthesis of Derivatives of Hydrazones (**3a–3j**)

For the synthesis of hydrazides (**3a–3j**), we took equal amounts of phenyl acetohydrazine (**2**) (Scheme 1 of Figure 2) or benzohydrazine (0.1 mmol, **3**, Scheme 2 of Figure 2) and various substituted aldehydes (**1a–1j**) in a round-bottom flask containing a catalytic amount of chitosan hydrochloride (20% *w*/*w*)/ethanol (Figure 2) [6,7]. This reaction mixture was stirred at room temperature until completion. The crude solid products obtained were then washed with cold alcohol and characterized. All reactions were completed within 15–20 min. The spectral data for synthesized compounds is available in the supporting information.

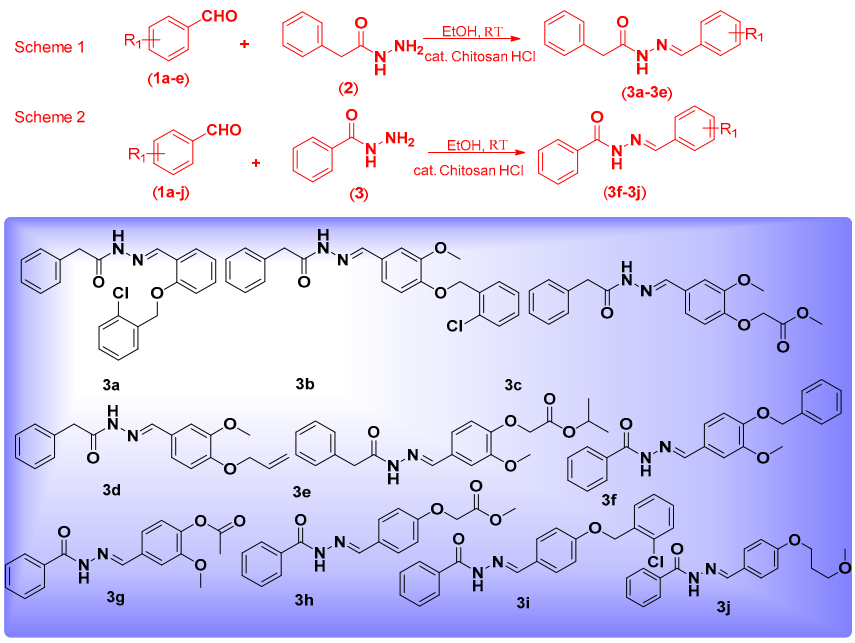

Figure 2. Schematic representation of employed synthesis schemes and studied hydrazide derivatives (**3a**–**3j**).

2.3. Molecular Docking and Theoretical Analysis

The structures of all compounds were drawn using 'ChemDraw V. 12.1′ and converted into 3D formats. The optimized structures were then docked using the 'Glide' module from Schrodinger, LLC, (New York, NY, USA) NY suite, 2021 [8]. All 3D crystal structures for docking were downloaded from the protein database bank (PDB database, www.rcsb.org, accessed on 10 October 2021) [9]. Docking was carried out using known protocols (Table 1) [1,2]. The gas-phase structures of the synthesized compounds (shown in Figure 3) were optimized by means of density functional theory (DFT). The DFT calculation was performed by the hybrid B3LYP method, which is based on the idea of Becke and considers a mixture of the exact (HF) and DFT exchange utilizing the B3 functional, together with the LYP correlation functional. The B3LYP calculations were performed in conjunction with the basis set 6-311++G** (Table 2) [1].

Table 1. Glide docking score for the best docked molecule, **3e**, along with interacted amino acid residues against various antimicrobial targets.

Sr. No.	Target (PDB Id)	Residues with Contribution Energy (kcal/mol)
1	1ai9 (*Candida albicans* dihydrofolate reductase)	LYS 57, ALA 115, THR 58, ARG 56 (−7.2)
2	1d7u (2,2-dialkylglycine decarboxylase)	ARG406, LYS 272, ASN 394, SER 271, TRP 138 (−9.746)
3	2x22 (enoyl acyl carrier enzyme)	ALA191, PRO 193, THR 196, MET 199, ILE 202, TRP 222 (−8.32)
4	2xcs (*S. aureus* Gyrase complex)	DG E:10, DC E:11, DG F:10, DC F:11 (−5.47)
5	3ivx (*mycobacterial* pantothenate synthase)	GLN 72, TYR 82, LYS 160, HIS 47, THR 186, VAL 184, VAL 187, ALA 49 (−9.23)

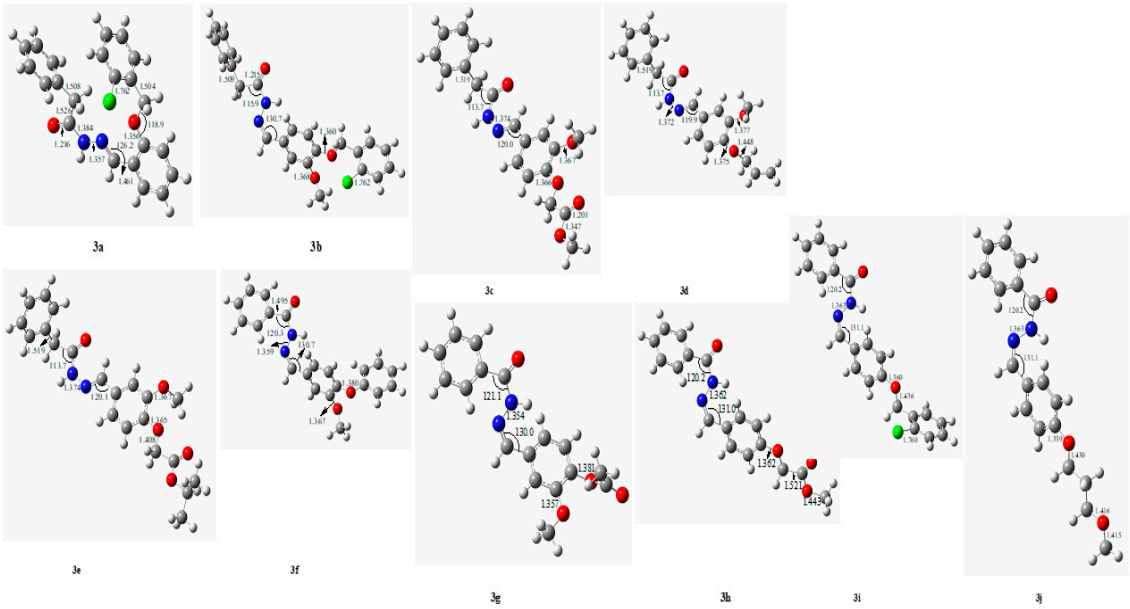

Figure 3. The B3LYP-optimized geometries of **3a**–**3j** (bond lengths in Å and bond angles).

Table 2. Calculated quantum chemical descriptors.

Comp. Id	EHOMO (eV)	ELUMO (eV)	Gap, D (Debye)	μ (eV)	η (eV)	S (eV-1)	ω (eV)
3a	−6.0906	−1.6796	4.7314	3.8851	2.2055	0.4534	3.4219
3b	−6.2155	−1.5537	5.8692	3.8846	2.3309	0.4290	3.2369
3c	−5.8994	−1.5409	5.1159	3.7201	2.1793	0.4589	3.1753
3d	−6.1532	−1.6587	1.7175	3.9059	2.2473	0.4450	3.3944
3e	−5.8632	−1.5153	5.3443	3.6893	2.1740	0.4600	3.1304
3f	−6.5476	−1.8888	3.7701	4.2182	2.3294	0.4293	3.8192
3g	−6.6409	−2.0006	5.4182	4.3207	2.3202	0.4310	4.0231
3h	−6.3164	−1.6927	6.3137	4.0045	2.3119	0.4326	3.4682
3i	−6.2147	−1.6233	5.2590	3.9190	2.29568	0.4356	3.3451
3j	−6.2198	−1.6279	6.1410	3.9239	2.2960	0.4355	3.3530

2.4. The 96-Well Microplate Alamar Blue Assay (MABA) Study and Plausible Mechanism for Anti-TB Activity

The 96-well Microplate Alamar Blue Assay (MABA) allows for the quantitative determination of drug susceptibility against any strain of replicating Mycobacterium tuberculosis to be completed within a week at minimal cost. The observed blue color indicated mycobacterial growth inhibition at a particular concentration of the particular wells. All our synthesized compounds were found to possess moderate anti-TB activity (a minimum of 100 μg/mL of minimum inhibitory concentration (MIC) values) when tested using the microplate Alamar Blue assay (MABA) (Repetitions, n = 3).

3. Results and Discussion

3.1. Docking Studies

Based on the microbial activity of hydrazides derivatives, it seemed reasonable to conduct a molecular docking study with the enzyme dialkylglycine decarboxylate (DGD). The DGD is a pyridoxal-5′-phosphate (PLP)-dependent enzyme that can catalyze both decarboxylation and transamination in its normal catalytic cycle. There are several evidences derived from molecular modeling studies and experimental data demonstrating how these inhibitors bind to the active site of 2,2-dialkylglycine decarboxylase (DGD) [18]. Pantothenate biosynthesis is essential for the virulence of *Mycobacterium tuberculosis*, and

this pathway thus presents potential drug targets against tuberculosis. We determined the crystal structure of pantothenate synthetase (PS) from *M. tuberculosis*, and its complexes with AMPCPP, pantoate, and a reaction intermediate, pantoyl adenylate, with resolutions from 1.6 to 2 Å. PS catalyzes the ATP-dependent condensation of pantoate and β-alanine to form pantothenate. Its structure reveals a dimer, and each subunit has two domains with a tight association between domains. All our synthesized compounds, **3a**–**3j**, were allowed to dock into the binding pockets of various antimicrobial targets such as the common antibacterial target 2,2-dialkylglycine decarboxylase (pdb id: 1d7u), *Candida albicans* dihydrofolate reductase (pdb id: 1ai9), *M. tuberculosis* InhA (pdb id: 2x22), the crystal structure of pantothenate synthetase (pdb id: 3ivx), etc. (Figure 4) [1]. The docking protocol was validated by redocking all in-bound ligands into active binding pockets of the respective crystal structures. The average RMSD value was retained to be around 2 Å. Our molecular docking analysis suggested that compound **3e** had the highest XP Gscore of −9.746 kcal/mol for the common antibacterial target (pdb id: 1d7u), indicating stronger antibacterial potentials. Compound **3e** interacted with *ASN394*, *ARG 406*, *LYS 272*, *SER 54*, *SER 215* amino acid residues from target 1d7u. The detailed binding scores (kcal/mol) and interacting residues for the best docked molecule **3e** are provided in Table 1.

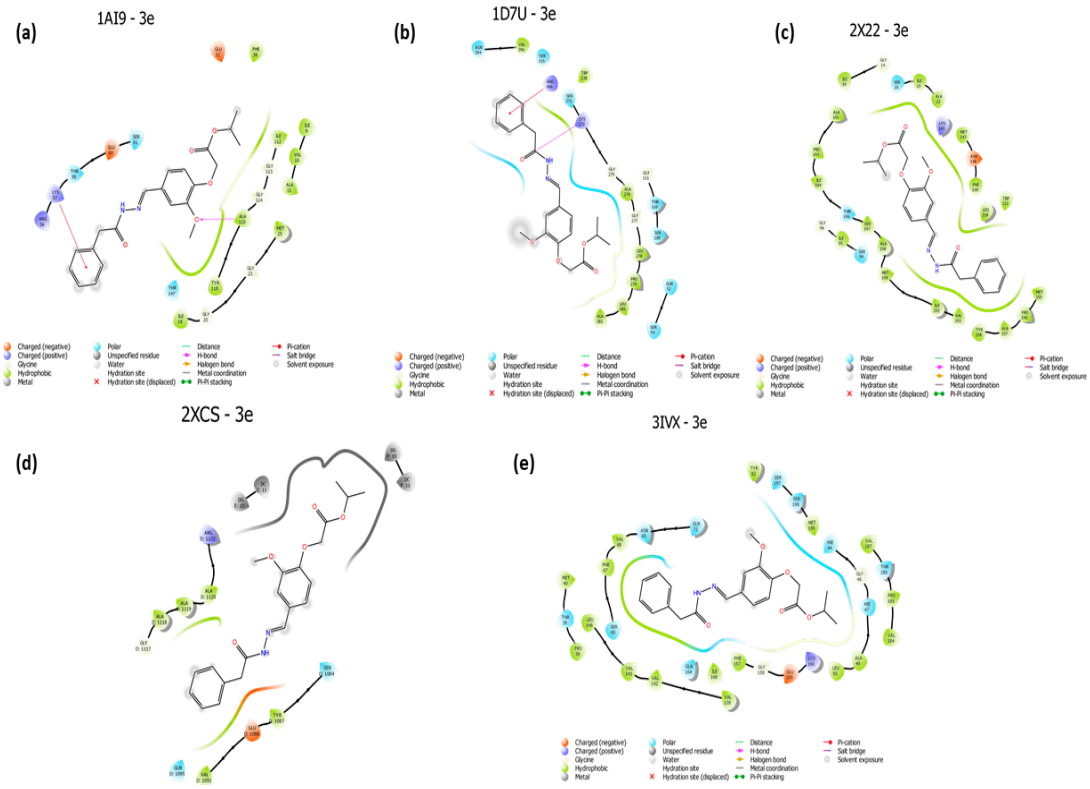

Figure 4. Docking interaction diagrams for best docked, **3e**, against various microbial targets, (**a**) 1ai9, (**b**) 1d7u, (**c**) 2x22, (**d**) 2xcs and (**e**) 3ivx.

3.2. Theoretical Analysis

The B3LYP-converged geometries of the studied compounds are summarized in Figures 3–5. The energy of the highest occupied molecular orbital (E_{HOMO}), the energy of the lowest unoccupied molecular orbital (E_{LUMO}), dipole moment (D), and the quantum chemical descriptors including the chemical potential (μ), chemical hardness (η), softness (S), and electrophilicity index (ω) are calculated by known equations (Supporting Material) [1], where I and A are the ionization energy and electron affinity of a species, respectively. Furthermore, the ionization energy (I) and the electron affinity (A) of a species could be calculated by applying the Koopmans' theory ($I = -E_{HOMO}$ and $A = -E_{LUMO}$),

and the quantum chemical descriptors were calculated and summarized in Table 2. The stability and reactivity of molecules are significantly related to their chemical hardness and global softness [1]. The smaller (greater) the value of hardness (softness) that a molecule has, the more reactive it should be. From Table 2, it was observed that **3e** exhibited the lowest value of chemical hardness and highest value of global softness among the studied compounds; therefore, it is chemically more reactive and less stable than all other compounds. According to the previous relevant studies [10,11], the toxicity of a species seems to be correlated with its electrophilicity index (ω). From Table 2, it was observed that **3e** showed the lowest value of the electrophilicity index (ω) among the tested compounds, which indicates that it should have the lowest toxicity among all the studied compounds [11]. Figure 4 depicts the HOMO and LUMO diagrams for the best docked molecule **3e**.

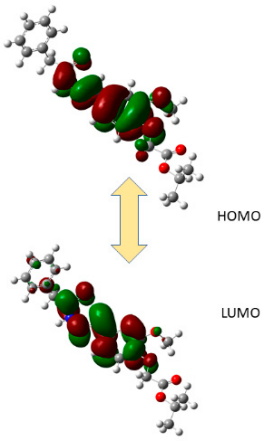

Figure 5. Highest occupied molecular orbital (HOMO) and lowest unoccupied molecular orbitals (LUMO) of **3e**.

4. Conclusions

In the current study, we have successfully synthesized various hydrazide derivatives (**3a**–**3j**) using a greener catalyst (chitosan HCl). The reaction was accompanied with minimal use of solvents and fewer workups. Considering the abundancy of raw unmodified chitosan, chitosan-HCl-mediated reactions may strengthen newer aspects of greener reactions. Hydrazide-hydrazones are typically reported on for their potent antimicrobial potentials. Currently synthesized analogues (**3a**–**3j**) showed higher binding scores against common bacterial targets. Moreover, our DFT calculations depicted that compound **3e** had better theoretical properties. Combining in silico docking and DFT results, compound **3e** may serve as the future hit/lead molecule for the development of potent antimicrobial agents.

Supplementary Materials: The following are available online at https://www.mdpi.com/article/10.3390/ecsoc-25-11655/s1. Experimental details.

Author Contributions: Conceptualization, S.N.M. and B.R.T.; methodology, B.R.T.; software, S.N.M. and C.-H.L.; writing—review and editing, A.P., B.R.T., S.N.M. and C.-H.L.; visualization, S.N.M. and A.P.; supervision, A.P. All authors have read and agreed to the published version of the manuscript.

Funding: We wish to thank the Dept. of Pharmaceutical Sciences, Birla Institute of Technology, Mesra, India for financial assistance. SM is also thankful for the provision of IRF (PHD/PH/10006/20) (Ref. No. GO/Estb/Ph.D./IRF/2020-21/) provided by BIT, Mesra, India.

Institutional Review Board Statement: Not applicable.

Informed Consent Statement: Not applicable.

Data Availability Statement: Not applicable.

Acknowledgments: The authors would like to thank the Head of the Department of Pharmaceutical Sciences and Technology, BIT, Mesra and Department of Chemistry, Government of Maharashtra's Ismail Yusuf College of Arts, Science and Commerce, Mumbai–60 for providing the research facilities for performing the current study. The author, SM is thankful to the Schrodinger team, Bangalore, India for providing a trial version of the Schrodinger suite for his thesis research work.

Conflicts of Interest: The authors declare no conflict of interest.

References

1. Mishra, V.R.; Ghanavatkar, C.W.; Mali, S.N.; Qureshi, S.I.; Chaudhari, H.K.; Sekar, N. Design, synthesis, antimicrobial activity and computational studies of novel azo linked substituted benzimidazole, benzoxazole and benzothiazole derivatives. *Comput. Biol. Chem.* **2019**, *78*, 330–337. [CrossRef] [PubMed]
2. Kshatriya, R.; Kambale, D.; Mali, S.; Jejurkar, V.P.; Lokhande, P.; Chaudhari, H.K.; Saha, S.S. Brønsted acid catalyzed domino synthesis of functionalized 4H-chromens and their ADMET, molecular docking and antibacterial studies. *ChemistrySelect* **2019**, *4*, 7943–7948. [CrossRef]
3. Jadhav, B.S.; Yamgar, R.S.; Kenny, R.S.; Mali, S.N.; Chaudhari, H.K.; Mandewale, M.C. Synthesis, In silico and Biological Studies of Thiazolyl-2h-chromen-2-one Derivatives as Potent Antitubercular Agents. *Curr. Comput.-Aided Drug Des.* **2020**, *16*, 511–522. [CrossRef]
4. Desale, V.J.; Mali, S.N.; Chaudhari, H.K.; Mali, M.C.; Thorat, B.R.; Yamgar, R.S. Synthesis and Anti-mycobacterium Study on Halo-substituted 2-aryl oxyacetohydrazones. *Curr. Comput.-Aided Drug Des.* **2020**, *16*, 618–628. [CrossRef] [PubMed]
5. Shelke, P.B.; Mali, S.N.; Chaudhari, H.K.; Pratap, A.P. Chitosan hydrochloride mediated efficient, green catalysis for the synthesis of perimidine derivatives. *J. Heterocycl. Chem.* **2019**, *56*, 3048–3054. [CrossRef]
6. Thorat, B.R.; Rani, D.; Yamgar, R.S.; Mali, S.N. Synthesis, Spectroscopic, In-vitro and Computational Analysis of Hydrazones as Potential Antituberculosis Agents:(Part-I). *Comb. Chem. High Throughput Screen.* **2020**, *23*, 392–401. [CrossRef]
7. Thorat, B.R.; Mali, S.N.; Rani, D.; Yamgar, R.S. Synthesis, In silico and In vitro Analysis of Hydrazones as Potential Antituberculosis Agents. *Curr. Comput.-Aided Drug Des.* **2021**, *17*, 294–306. [CrossRef]
8. *Glide*; Schrodinger, LLC.: New York, NY, USA, 2021.
9. The Protein Database Bank, PDB Database. Available online: www.rcsb.org (accessed on 10 October 2021).
10. Mali, S.N.; Pandey, A. Balanced QSAR and Molecular Modeling to Identify Structural Requirements of Imidazopyridine Analogues as Anti-infective Agents against Trypanosomiases. *J. Comput. Biophys. Chem.* **2021**, *21*, 83–114. [CrossRef]
11. Mishra, V.R.; Ghanavatkar, C.W.; Mali, S.N.; Chaudhari, H.K.; Sekar, N. Schiff base clubbed benzothiazole: Synthesis, potent antimicrobial and MCF-7 anticancer activity, DNA cleavage and computational study. *J. Biomol. Struct. Dyn.* **2019**, *38*, 1772–1785. [CrossRef]
12. Jejurkar, V.P.; Mali, S.N.; Kshatriya, R.; Chaudhari, H.K.; Saha, S. Synthesis, antimicrobial screening and in silico appraisal of iminocarbazole derivatives. *ChemistrySelect* **2019**, *4*, 9470–9475. [CrossRef]
13. Anuse, D.G.; Mali, S.N.; Thorat, B.R.; Yamgar, R.S.; Chaudhari, H.K. Synthesis, SAR, in silico appraisal and anti-microbial study of substituted 2-aminobenzothiazoles derivatives. *Curr. Comput.-Aided Drug Des.* **2020**, *16*, 802–813. [CrossRef] [PubMed]
14. Mali, S.N.; Pandey, A. Molecular modeling studies on 2,4-disubstituted imidazopyridines as anti-malarials: Atom-based 3D-QSAR, molecular docking, virtual screening, in-silico ADMET and theoretical analysis. *J. Comput. Biophys. Chem.* **2021**, *20*, 267–282. [CrossRef]
15. Kapale, S.S.; Mali, S.N.; Chaudhari, H.K. Molecular modelling studies for 4-oxo-1,4-dihydroquinoline-3-carboxamide derivatives as anticancer agents. *Med. Drug Discov.* **2019**, *2*, 100008. [CrossRef]
16. Desale, V.J.; Mali, S.N.; Thorat, B.R.; Yamgar, R.S. Synthesis, admetSAR Predictions, DPPH Radical Scavenging Activity, and Potent Anti-mycobacterial Studies of Hydrazones of Substituted 4-(anilino methyl) benzohydrazides (Part 2). *Curr. Comput.-Aided Drug Des.* **2021**, *17*, 493–503. [CrossRef]
17. Kshatriya, R.; Shelke, P.; Mali, S.; Yashwantrao, G.; Pratap, A.; Saha, S. Synthesis and evaluation of anticancer activity of pyrazolone appended triarylmethanes (TRAMs). *ChemistrySelect* **2021**, *6*, 6230–6239. [CrossRef]
18. Mali, S.N.; Pandey, A. Multiple QSAR and molecular modelling for identification of potent human adenovirus inhibitors. *J. Indian Chem. Soc.* **2021**, *98*, 100082. [CrossRef]
19. Mali, S.N.; Thorat, B.R.; Gupta, D.R.; Pandey, A. Mini-Review of the Importance of Hydrazides and Their Derivatives—Synthesis and Biological Activity. *Eng. Proc.* **2021**, *11*, 21.
20. Mali, S.N.; Pandey, A.; Thorat, B.R.; Lai, C.H. Multiple 3D-and 2D-quantitative structure–activity relationship models (QSAR), theoretical study and molecular modeling to identify structural requirements of imidazopyridine analogues as anti-infective agents against tuberculosis. *Struct. Chem.* **2022**, *33*, 679–694. [CrossRef]
21. Nagre, D.T.; Mali, S.N.; Thorat, B.R.; Thorat, S.A.; Chopade, A.R.; Farooqui, M.; Agrawal, B. Synthesis, In-Silico Potential Enzymatic Target Predictions, Pharmacokinetics, Toxicity, Anti-Microbial and Anti-Inflammatory Studies of Bis-(2-Methylindolyl) Methane Derivatives. *Curr. Enzym. Inhib.* **2021**, *17*, 127–143. [CrossRef]
22. Ghosh, S.; Mali, S.N.; Bhowmick, D.N.; Pratap, A.P. Neem oil as natural pesticide: Pseudo ternary diagram and computational study. *J. Indian Chem. Soc.* **2021**, *98*, 100088. [CrossRef]

23. Mali, S.N.; Tambe, S.; Pratap, A.P.; Cruz, J.N. Molecular Modeling Approaches to Investigate Essential Oils (Volatile Compounds) Interacting with Molecular Targets. In *Essential Oils*; Santana de Oliveira, M., Ed.; Springer: Berlin/Heidelberg, Germany, 2022; Volume 1, pp. 417–442. [CrossRef]
24. Mali, S.N.; Pandey, A. Synthesis of New Hydrazones using a biodegradable catalyst, their Biological Evaluations and Molecular Modeling Studies (Part-II). *J. Comput. Biophys. Chem.* **2022**. [CrossRef]
25. Macquarrie, D.J.; Hardy, J.J. Applications of functionalized chitosan in catalysis. *Ind. Eng. Chem. Res.* **2005**, *44*, 8499–8520. [CrossRef]
26. Antony, R.; Arun, T.; Manickam, S.T.D. A review on applications of chitosan-based Schiff bases. *Int. J. Biol. Macromol.* **2019**, *129*, 615–633. [CrossRef] [PubMed]
27. El Kadib, A. Chitosan as a sustainable organocatalyst: A concise overview. *ChemSusChem* **2015**, *8*, 217–244. [CrossRef]
28. Godiya, C.B.; Revadekar, C.; Kim, J.; Park, B.J. Amine-bilayer-functionalized cellulose-chitosan composite hydrogel for the efficient uptake of hazardous metal cations and catalysis in polluted water. *J. Hazard. Mater.* **2022**, *436*, 129112. [CrossRef] [PubMed]
29. Badgujar, V.C.; Bhanage, B.M. Recent update on use of ionic liquids for enzyme immobilization, activation and catalysis: A partnership for sustainability. *Curr. Opin. Green Sustain. Chem.* **2022**, *36*, 100621. [CrossRef]